Diabetes Reduces Severity of Aortic Aneurysms Depending on the Presence of Cell Division Autoantigen 1 (CDA1)

Jiaze Li,[1,2,3] Pacific Huynh,[1,2,3] Aozhi Dai,[1,3] Tieqiao Wu,[1,3] Yugang Tu,[3] Bryna Chow,[1,3] Helen Kiriazis,[4] Xiao-Jun Du,[4] Leon A. Bach,[5,6] Jennifer L. Wilkinson-Berka,[1] Erik Biros,[7] Philip Walker,[8†] Maria Nataatmadja,[7,8] Malcolm West,[7,8] Jonathan Golledge,[7,8,9] Terri J. Allen,[1,3] Mark E. Cooper,[1,2,3] and Zhonglin Chai[1,2,3]

Diabetes 2018;67:755–768 | https://doi.org/10.2337/db17-0134

Diabetes is a negative risk factor for aortic aneurysm, but the underlying explanation for this phenomenon is unknown. We have previously demonstrated that cell division autoantigen 1 (CDA1), which enhances transforming growth factor-β signaling, is upregulated in diabetes. We hypothesized that CDA1 plays a key role in conferring the protective effect of diabetes against aortic aneurysms. Male wild-type, CDA1 knockout (KO), apolipoprotein E (ApoE) KO, and CDA1/ApoE double-KO (dKO) mice were rendered diabetic. Whereas aneurysms were not observed in diabetic ApoE KO and wild-type mice, 40% of diabetic dKO mice developed aortic aneurysms. These aneurysms were associated with attenuated aortic transforming growth factor-β signaling, reduced expression of various collagens, and increased aortic macrophage infiltration and matrix metalloproteinase 12 expression. In the well-characterized model of angiotensin II–induced aneurysm formation, concomitant diabetes reduced fatal aortic rupture and attenuated suprarenal aortic expansion, changes not seen in dKO mice. Furthermore, aortic CDA1 expression was downregulated ∼70% within biopsies from human abdominal aortic aneurysms. The identification that diabetes is associated with upregulation of vascular CDA1 and that CDA1 deletion in diabetic mice promotes aneurysm formation provides evidence that CDA1 plays a role in diabetes to reduce susceptibility to aneurysm formation.

Aortic aneurysm is a major cause of mortality in older adults (1). Interestingly, although diabetes is associated with an increased incidence of cardiovascular disease, specifically related to atherosclerosis, the incidence of aortic aneurysms has been reported to be reduced in diabetes (2–5). The underlying mechanisms for this puzzling clinical observation are poorly understood (2,6). Diabetic complications are considered to be closely linked to enhanced transforming growth factor-β (TGF-β) signaling (7–11). Aneurysm formation is thought to occur as a result of altered

[1]Department of Diabetes, Central Clinical School, Monash University, Melbourne, Australia
[2]Department of Immunology, Central Clinical School, Monash University, Melbourne, Australia
[3]Diabetes Division, Baker IDI Heart and Diabetes Institute, Melbourne, Australia
[4]Experimental Cardiology Laboratory, Baker IDI Heart and Diabetes Institute, Melbourne, Australia
[5]Department of Medicine, Central Clinical School, Monash University, Melbourne, Australia
[6]Department of Endocrinology and Diabetes, Alfred Hospital, Melbourne, Australia
[7]Vascular Biology Unit, Queensland Research Centre for Peripheral Vascular Disease, James Cook University, Townsville, Australia
[8]University of Queensland, Brisbane, Australia
[9]Department of Vascular and Endovascular Surgery, Townsville Hospital, Townsville, Australia

Corresponding authors: Zhonglin Chai, zhonglin.chai@monash.edu, and Jonathan Golledge, jonathan.golledge@jcu.edu.au.

Received 31 January 2017 and accepted 1 January 2018.

This article contains Supplementary Data online at http://diabetes.diabetesjournals.org/lookup/suppl/doi:10.2337/db17-0134/-/DC1.

J.L., P.H., and A.D. contributed equally to this work.

P.H., A.D., T.W., B.C., T.J.A., M.E.C., and Z.C. are currently affiliated with the Department of Diabetes, Central Clinical School, Monash University, Melbourne, Australia.

†Deceased.

TGF-β signaling, enhanced inflammation, and activation of matrix metalloproteinases (MMPs), which leads to increased degradation of extracellular matrix (ECM) and weakening of the vessel wall (12,13). Genetic mutations and impaired functions of genes involved in the TGF-β signaling pathway have been demonstrated to play a causal role in aortic aneurysm formation (14–22). We have previously shown that cell division autoantigen 1 (CDA1) is upregulated in diabetes and enhances TGF-β signaling, including in the vasculature (23–25). Based on these findings, we postulated a role for CDA1 in promoting resistance to aneurysm formation in diabetes. In the current study, we have directly examined if CDA1 contributes to the relative protection from aortic aneurysm associated with diabetes using various models of aneurysm formation in the setting of concurrent streptozotocin-induced diabetes in mice with and without deletion of CDA1, a molecule implicated in TGF-β signaling.

RESEARCH DESIGN AND METHODS

Mice With and Without Diabetes

The CDA1 knockout (KO) and the CDA1/apolipoprotein E (ApoE) double-KO (dKO) mouse strains, both on a C57BL/6 background, have been previously described (25). In this study, male wild-type (WT), CDA1 KO, and ApoE KO and dKO mice were rendered diabetic by five consecutive daily injections with streptozotocin (55 mg/kg) or injected with buffer alone to serve as nondiabetic controls. Animals were euthanized 20 weeks later for analysis of aortic tissues and metabolic parameters as previously described (23–25). The animal studies were approved by the Alfred Medical Research and Education Precinct Animal Ethics Committee.

Morphometric Determination of Aortic Size and Histological and Biochemical Analyses

Aortas were dissected and placed in cold 0.9% sodium chloride and photographed. A subset of aortas was either fixed in 10% neutral buffered formalin for histological analysis or snap frozen in liquid nitrogen for later extraction of total RNA. The maximum diameters of the ascending, descending, and abdominal aortas were determined by analysis of the photographed images as previously described (26). Measurements were taken in duplicate in a blinded fashion.

Assessment of Aortic Aneurysm

Aortic aneurysms were assessed by three techniques in different experiments. Firstly, isolated aortas were photographed and morphometrically examined (see above). Secondly, aortas were examined histologically for areas of balloon-like bulges under the microscope at a magnification ×10. Histological features of aneurysm such as medial elastin lamella breaks, adventitial structural damage, and macrophage infiltration were sought (27). Thirdly, aortas were examined in vivo using ultrasound imaging, and the maximum aortic diameters were determined at the suprarenal region (see below).

Analysis of Aortic Elastin Lamella and Collagen Fibril Structure

Paraffin-embedded aortic sections (4-μm thick) were stained in orcein solution and counterstained by hematoxylin and eosin (H&E) as previously described (28). The degree of elastin lamella fragmentation was graded by an observer blinded to the mouse group using a scoring system (scores 0–4) previously used (29,30). Examples of each grade are illustrated in Supplementary Fig. 1. Elastin lamella thickness of each sample was randomly measured at 10 random locations using Photoshop CS4 software (Adobe Systems). Aortic collagen staining using picrosirius red (31) and confocal microscopy examination of the collagen fiber network (32) have been previously described. Picrosirius red–stained collagen fiber images were analyzed for fiber anisotropy using the Fibriltool plugin in ImageJ software (National Institutes of Health) as described previously (33).

Immunohistochemical Staining

Paraffin-embedded aortic sections were immunohistochemically stained for various fibrotic and inflammatory proteins, and the staining signals were quantified as previously described (24,25). For phospho-Smad3 staining, the percentage of cells with positively stained nuclei among cells examined were quantified. Antibodies to collagen III (ab7778), phospho-Smad3 (ab52903), and F4/80 (ab16911) were purchased from Abcam (Cambridge, U.K.), and antibody to collagen IV (GWB-5A65E0) was from GenWay Biotech (San Diego, CA). Negative control with no primary antibody and isotype control antibodies (Supplementary Fig. 2) was performed to confirm the specificity of the immunohistochemical staining.

Determination of mRNA Levels in Mouse Aortas

Gene-specific mRNA levels were determined by real-time RT-PCR as previously described (24,25). RT-PCR was carried out on the cDNA templates using TaqMan Fast Universal PCR Master Mix (Applied Biosystems, Foster City, CA) with β-actin gene used as an internal control. The sequences of primers and probes are shown in Supplementary Table 1.

Angiotensin II Infusion in Nondiabetic and Diabetic Mice

To further explore the role of diabetes and CDA1 expression, a well-characterized model of aortic aneurysm formation was studied, involving angiotensin II (AngII) infusion (34). Male mice were rendered diabetic by streptozotocin as described above. Ten weeks later, both nondiabetic and diabetic mice were implanted with an Alzet osmotic minipump (model 1004; Alzet, Cupertino, CA) subcutaneously, which released AngII at a dose of 1 μg/min/kg for 4 weeks. Animals found dead were autopsied in order to identify any evidence of aortic aneurysm rupture as well as the rupture site. Animals found to be severely sick, which had to be killed according to the animal welfare guidelines, were included as censored in the survival curve comparison analysis. Animals were killed after 4 weeks' AngII infusion, and their aortas were examined for the assessment of aortic aneurysms. Isolated aortas were photographed before being

either fixed in formalin for subsequent histology or frozen for further analysis.

Measurement of Inner Diameter of the Suprarenal Aorta in Live Animals

Ultrasound imaging examination was performed on animals receiving AngII infusion in order to analyze the size of the abdominal aorta (35). Animals were examined on the same day or <2 days before AngII infusion started in order to measure the baseline diameter as well as at weeks 1 and 2 after AngII infusion in order to detect the changes in aortic diameter. High-resolution anterior–posterior images of motion-mode of aortas in isoflurane-anesthetized animals were recorded using the Vevo 2100 Imaging System with a 40-MHz probe (VisualSonics, Toronto, Ontario, Canada). The maximum inner wall to inner wall diameter of the suprarenal region of the aorta during systole was measured using the Vevo 2100 1.6.0 software.

Data Analysis

All of the data collected from the animal studies were analyzed by two-way ANOVA, and pairwise comparisons between experimental groups were performed using the Newman-Keuls test or by Fisher exact test. The D'Agostino-Pearson omnibus normality test was performed to check if the data were normally distributed. Survival curves were analyzed by Kaplan-Meier analysis and log-rank test. Any difference with $P < 0.05$ was defined as statistically significant.

Determination of Aortic CDA1 Gene Expression Levels in Human Abdominal Aortic Aneurysm Samples

In order to explore the role of CDA1 in human aneurysm formation, expression of the CDA1 gene was measured in human abdominal aortic aneurysm (AAA) biopsy samples. Ethics approval for the human sample work was obtained from the Townsville and the Royal Brisbane and Women's Hospitals' committees. Patients provided written informed consent. Abdominal aortic specimens were obtained from 15 patients undergoing open surgery to treat AAA and six organ donors. The maximum infrarenal aortic diameter was assessed in patients with AAA from axial computed tomography angiography images using the viewer function on a Philips workstation (MxView Visualization Workstation Software; Philips Electronics, Amsterdam, the Netherlands) as previously reported (36,37). The definitions of risk factors such as dyslipidemia, hypertension, diabetes, coronary heart disease, and smoking were as previously described (38). Full-thickness aortic wall biopsies were collected in RNAlater solution (Ambion, Waltham, MA) and stored at −80°C until assayed. The QuantiTect SYBR Green one-step RT-PCR Kit (Qiagen, Hilden, Germany) was used according to the manufacturer's instructions with 40 ng total RNA as template. All reactions were independently repeated in duplicate. QT00024353 and QT00095431 QuantiTect Primer Assays (Qiagen) were used to determine CDA1 and β-actin mRNA, respectively. CDA1 mRNA levels were calculated by using the concentration–threshold cycle standard curve method and normalized against the average expression of β-actin. The Mann–Whitney *U* test was performed to identify differences in CDA1 mRNA levels between AAA and control biopsies. Statistical significance was defined at the conventional 5% level.

RESULTS

Diabetic dKO Mice Were Prone to Aortic Aneurysm Formation

Metabolic parameters at 20 weeks after streptozotocin injections showed diabetes-associated changes in these mice as expected (Supplementary Table 2). No aneurysms were seen in diabetic WT or ApoE KO mice, but interestingly, aortic aneurysms were identified in 40% (10 out of 25) of diabetic dKO mice. Eight mice had solitary AAAs, and two mice had multiple aneurysms within the descending and abdominal aortas. Examples of these aneurysms are shown in Fig. 1*A*. Histological examination on five of the aortas with aneurysms demonstrated medial elastin lamellae fragmentation and macrophage infiltration in these aortas. No such bulges or histological features of aneurysm were observed in the diabetic ApoE KO mice ($n = 27$) (Fig. 1*B*) or in other groups (WT control, $n = 15$; WT diabetic, $n = 16$; CDA1 KO control, $n = 13$; CDA1 KO diabetic, $n = 17$; ApoE KO control, $n = 26$; dKO control, $n = 14$; $P < 0.003$ vs. diabetic dKO, Fisher exact test).

Diabetic dKO Mice Had Increased Aortic Diameters

A moderate increase in aortic diameter determined by the morphometric method was observed in the ascending (1.31 ± 0.02 vs. 1.20 ± 0.02 mm; $P < 0.002$) and descending (1.10 ± 0.12 vs. 0.84 ± 0.03 mm; $P = 0.036$) aortas of the diabetic dKO mice compared with the diabetic ApoE KO mice (Fig. 1*C* and *D*). A tendency toward an increase in the aortic diameter in the abdominal region (1.03 ± 0.10 vs. 0.88 ± 0.03 mm; $P = 0.13$) was also observed, although this difference was not statistically significant (Fig. 1*E*). Furthermore, WT and CDA1 KO mice on the C57BL/6 background, including both nondiabetic and diabetic groups, had no difference in aortic diameter (Supplementary Fig. 3).

Extensive Elastin Lamella Breakages at the Sites of Aortic Aneurysms

Histological examination of orcein- and H&E-stained aortic sections showed extensive breakage of the elastin lamella at the aneurysm site in diabetic dKO mice (Fig. 2). Diabetic ApoE KO mice developed atherosclerotic plaques within the intima (Fig. 2*A*). The diabetic dKO mice developed plaques invading into the media and adventitia, associated with breakage of elastin lamella at the affected site (Fig. 2*A*). An approximately twofold increase in the aortic elastin fragmentation in ApoE KO and dKO mice was observed when compared with WT and CDA1 KO mice (Fig. 2*B*). The diabetic dKO group had an ~30% greater elastin fragmentation compared with the diabetic ApoE KO group (Fig. 2*B*). The elastin lamella was thicker in diabetic ApoE KO mice. This parameter was significantly attenuated in the diabetic dKO mice (Fig. 2*C*).

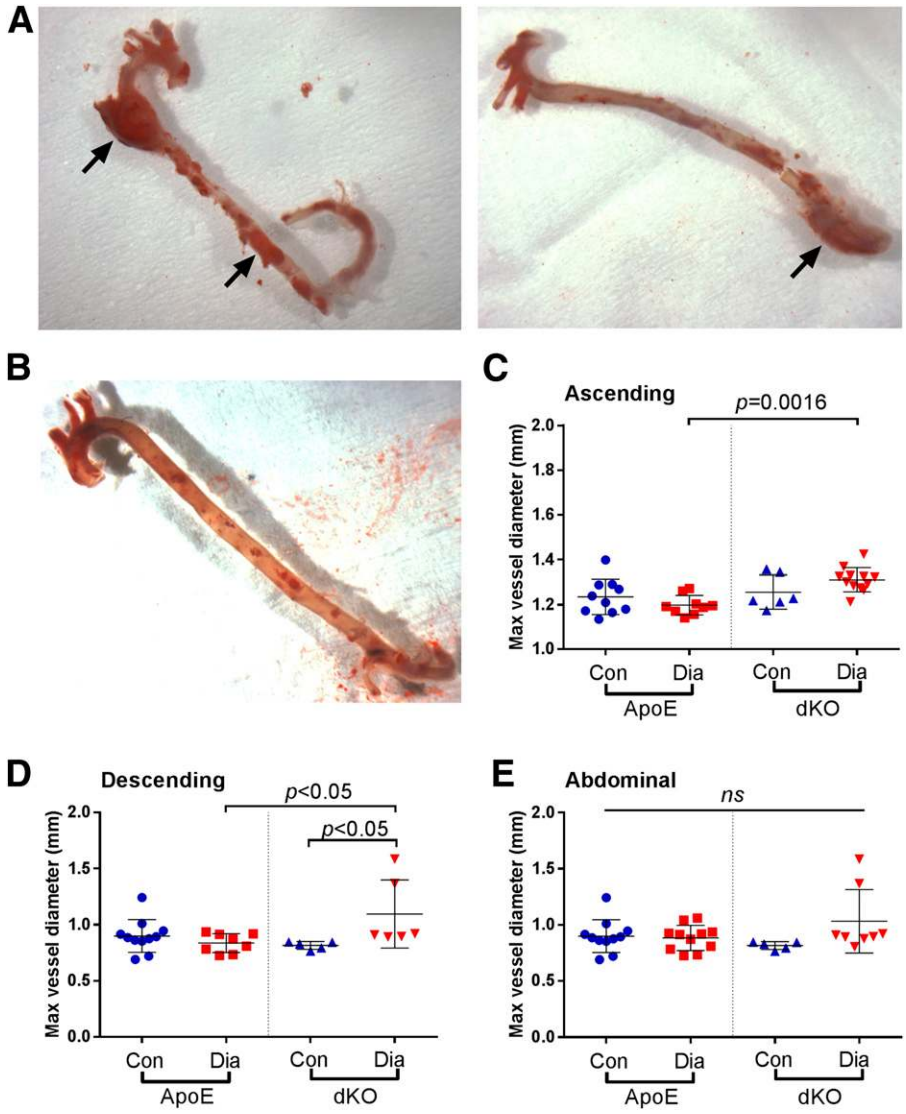

Figure 1—Aneurysms develop in diabetic dKO mice after 20 weeks of diabetes. *A*: Representative aortas from diabetic dKO mice show multiple aneurysms (arrows) at thoracic (left) and abdominal (right) sites. *B*: A representative aorta from a diabetic ApoE KO (ApoE) mouse shows no aneurysms. Aortic sizes (diameter) at ascending (*C*), descending (*D*), and abdominal (*E*) regions from control (Con) and diabetic (Dia) ApoE KO and diabetic dKO groups are shown as univariate scatterplots with mean ± SD and *P* value between specified groups.

CDA1 Deficiency Attenuated Diabetes-Associated Vascular Expression of ECM Genes Leading to Vascular ECM Remodeling

Aortic mRNA levels for collagens I and III were increased in diabetic ApoE KO mice compared with nondiabetic controls. Both of these parameters were significantly attenuated in the diabetic dKO mice (Fig. 3*A*). Immunohistochemical staining showed that aortic accumulation of collagens III (Fig. 3*B* and *C*) and IV (Fig. 3*D* and *E*) was greater in diabetic ApoE KO compared with nondiabetic mice, albeit the difference in quantification of collagen III staining failed to reach statistical significance. This effect of diabetes was significantly attenuated in the dKO mice. Picrosirius red staining showed that diabetic dKO mice aortas had lost the well-knitted collagen fiber structure within the aortic adventitia around the aneurysms (Fig. 4*A*). Collagen fiber structure within the medial layer of aortic aneurysms within the diabetic dKO mice was disorganized. This was consistent with the collagen fibril anisotropy finding, as assessed using ImageJ software (National Institutes of Health). A higher level of collagen fibril disarray at the lesion sites in the diabetic dKO mice has been observed, when compared with the diabetic ApoE KO mice (Fig. 4*B*). Confocal stacking images confirmed the disorganized collagen fiber network around the aneurysms in diabetic dKO mice (Fig. 4*C*).

TGF-β/Smad3 Signaling Was Attenuated in the Aortas of Diabetic dKO Mice

Nuclear staining of phospho-Smad3 in aortic sections by immunohistochemistry (Fig. 5*A*) showed a greater positive staining rate in diabetic ApoE KO mice compared with nondiabetic mice (>30 vs. ~13%; $P < 0.0001$). This parameter

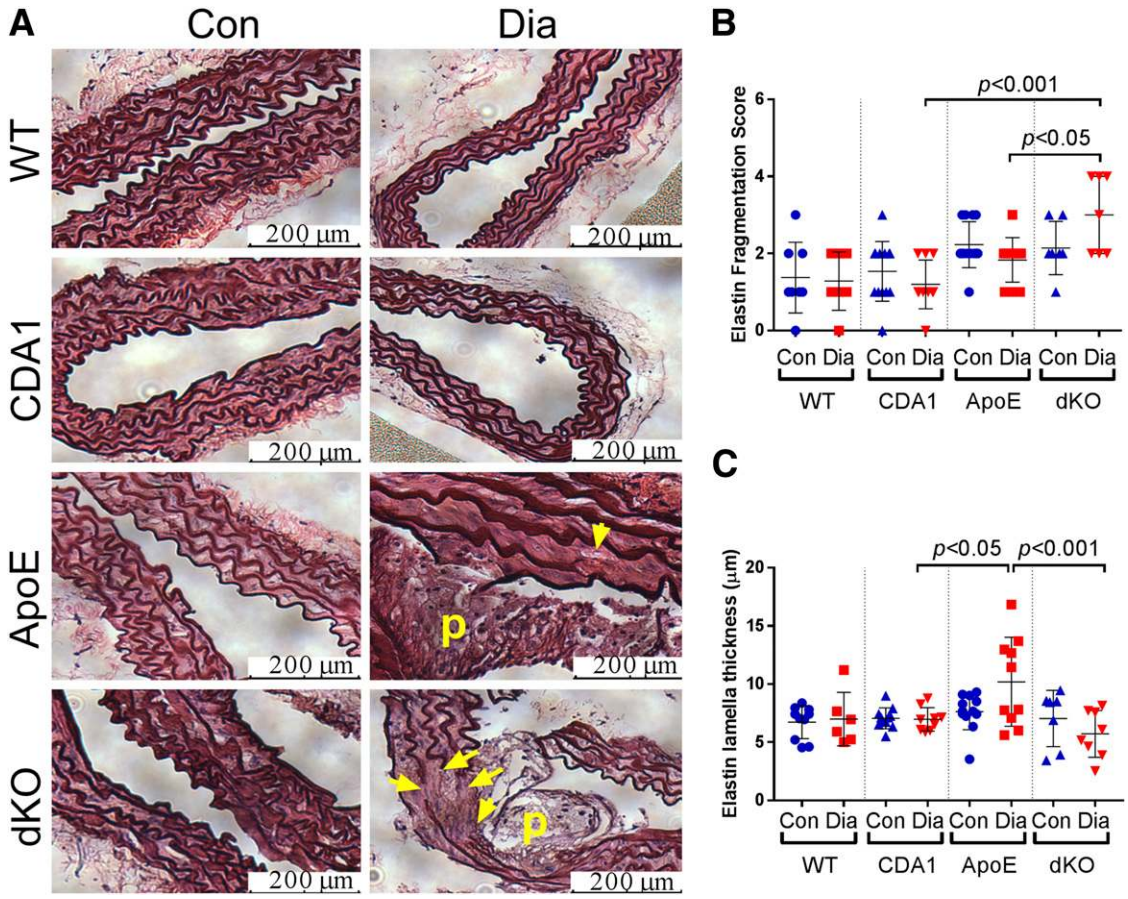

Figure 2—Extensive elastin lamella breaks at the aneurysm site. *A*: Ocein/H&E staining of aorta sections from 20-week diabetic (Dia) and age-matched nondiabetic control (Con) WT, CDA1 KO (CDA1), ApoE KO (ApoE), and CDA1/ApoE dKO (dKO) mice show elastin lamellae. Yellow arrows indicate the elastin lamella breaks. The atherosclerotic plaques are labeled (yellow "p"). Elastin fragmentation scores (*B*) and elastin lamella thickness (*C*) are shown as univariate scatterplots with mean ± SD and *P* value between specified groups.

was attenuated in diabetic dKO mice (~20%; $P < 0.0001$) (Fig. 5*B*). The effect of CDA1 on aortic phospho-Smad3 levels is further confirmed by Western blotting in 14-week diabetic and nondiabetic WT and CDA1 KO mice (Supplementary Fig. 4).

Diabetes and ApoE Deficiency Are Associated With Increased Aortic Macrophage Infiltration and MMP12 Expression

Mature macrophage marker, F4/80, was stained in aortas from diabetic ApoE KO (Fig. 6*A*) and dKO (Fig. 6*B*) mice with a twofold greater staining area observed in diabetic ApoE KO mice compared with controls (Fig. 6*C*, left panel). There was no statistically significant difference in F4/80 staining area between diabetic dKO and diabetic ApoE KO groups. Macrophages mainly accumulated within the atherosclerotic plaques in the intima of diabetic ApoE KO mice (Fig. 6*A*), whereas macrophages were abundantly present within the media as well as in the adventitia in the diabetic dKO mice at sites of aneurysms (Fig. 6*B*). When analyzing the macrophage staining distribution across the sectional layers of the aortic wall containing a plaque, the F4/80 immunohistochemical staining area in the medial-adventitial layers was approximately fivefold more than that seen in the intima in diabetic dKO mice, whereas there was more staining in the intima in the diabetic ApoE mice (Fig. 6*C*, right panel). The macrophage is known to be the main source of MMP12 within the vasculature, which is responsible for elastin degradation (39). Minimal MMP12 gene expression was detected in the WT and CDA1 KO groups. ApoE deficiency was associated with a >100-fold increase in aortic MMP12 mRNA levels in ApoE KO and dKO mice ($P < 0.05$) (Fig. 6*D*). Diabetes further increased the MMP12 mRNA levels in both strains of ApoE-deficient mice. MMP12 mRNA levels within macrophages isolated from the peritoneal cavity of ApoE KO and dKO mice were approximately fourfold higher than those of WT and CDA1 KO mice (Fig. 6*E*). These findings suggest that the infiltrating macrophages in the aorta of ApoE-deficient mice contributed to the increased activities of MMP12, leading to elastin degradation in the aortic wall.

Protective Effect of Diabetes in AngII-Induced Aneurysm in ApoE KO Mice Is CDA1 Dependent

Male ApoE KO and dKO mice injected with streptozotocin, monitored weekly, demonstrated blood glucose levels

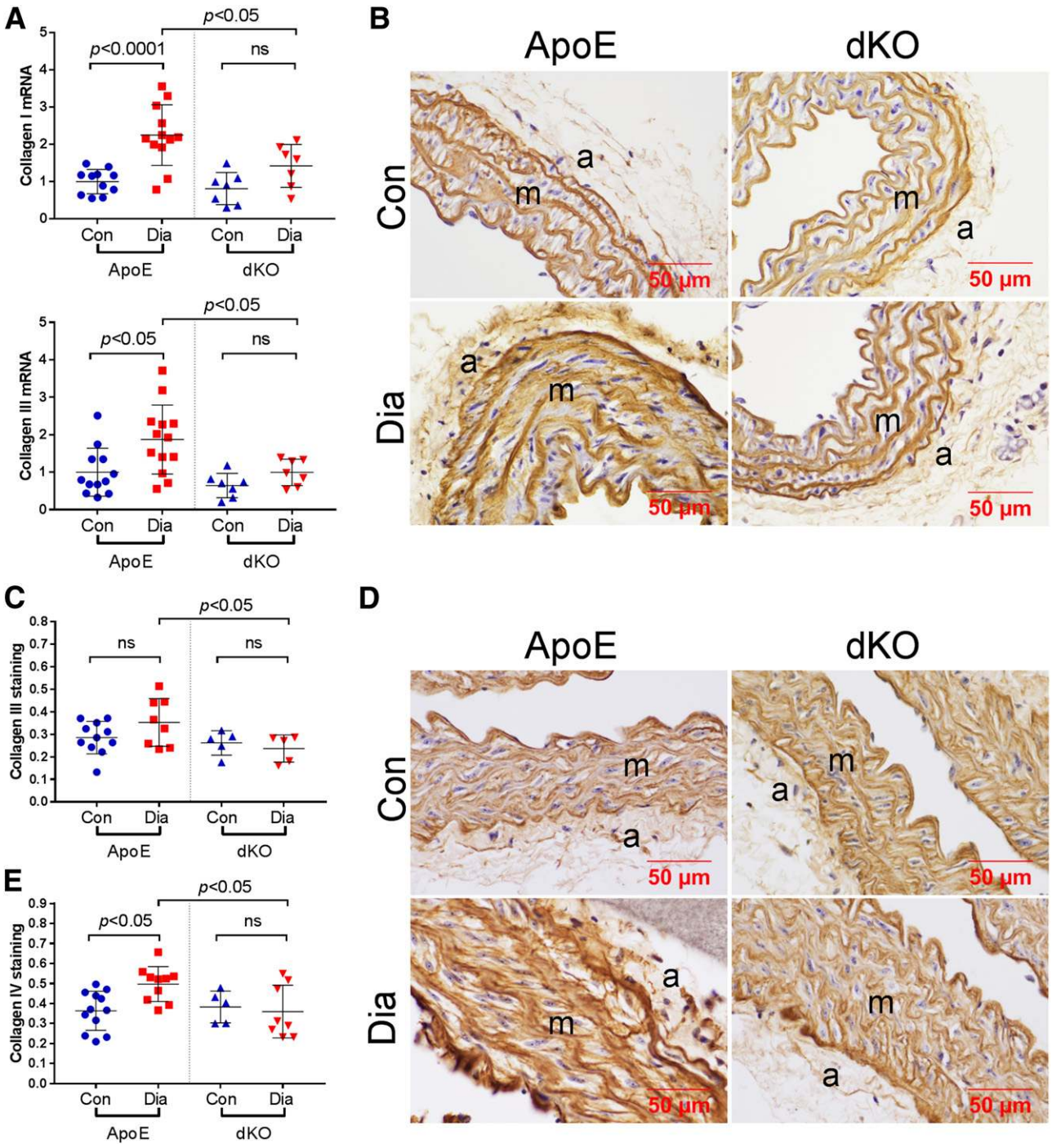

Figure 3—CDA1 deficiency attenuates diabetes-associated increases in aortic expression of collagens I, III, and IV. *A*: Aortic mRNA levels for collagens I and III in control (Con) and 20-week diabetic (Dia) ApoE KO (ApoE) and dKO groups are shown as univariate scatterplots with mean ± SD and *P* value between specified groups. *B–E*: Representative immunohistochemical staining for aortic collagens III (*B*) and IV (*D*) of these mice is shown. The quantification of the immunohistochemical staining for collagens III (*C*) and IV (*E*) is shown as individual value, mean ± SD, and *P* value between specified groups. a, adventitia; m, media.

>20 mmol/L, whereas mice injected with buffer alone had blood glucose levels of ~10 mmol/L. Ten weeks after streptozotocin injections, diabetic mice had lower body weight than controls (Supplementary Table 3). Both diabetic and control mice were given an AngII infusion for 4 weeks with the AngII dosage adjusted according to the body weight of individual mouse. The elevated HbA_{1c} levels seen in the diabetic mice and the blood pressure levels in all groups were not affected by the AngII infusion (Supplementary Table 3). Approximately 53% (9 out of 17) of nondiabetic ApoE KO mice died of aortic aneurysm rupture, occurring on days 3–13 during the AngII infusion,

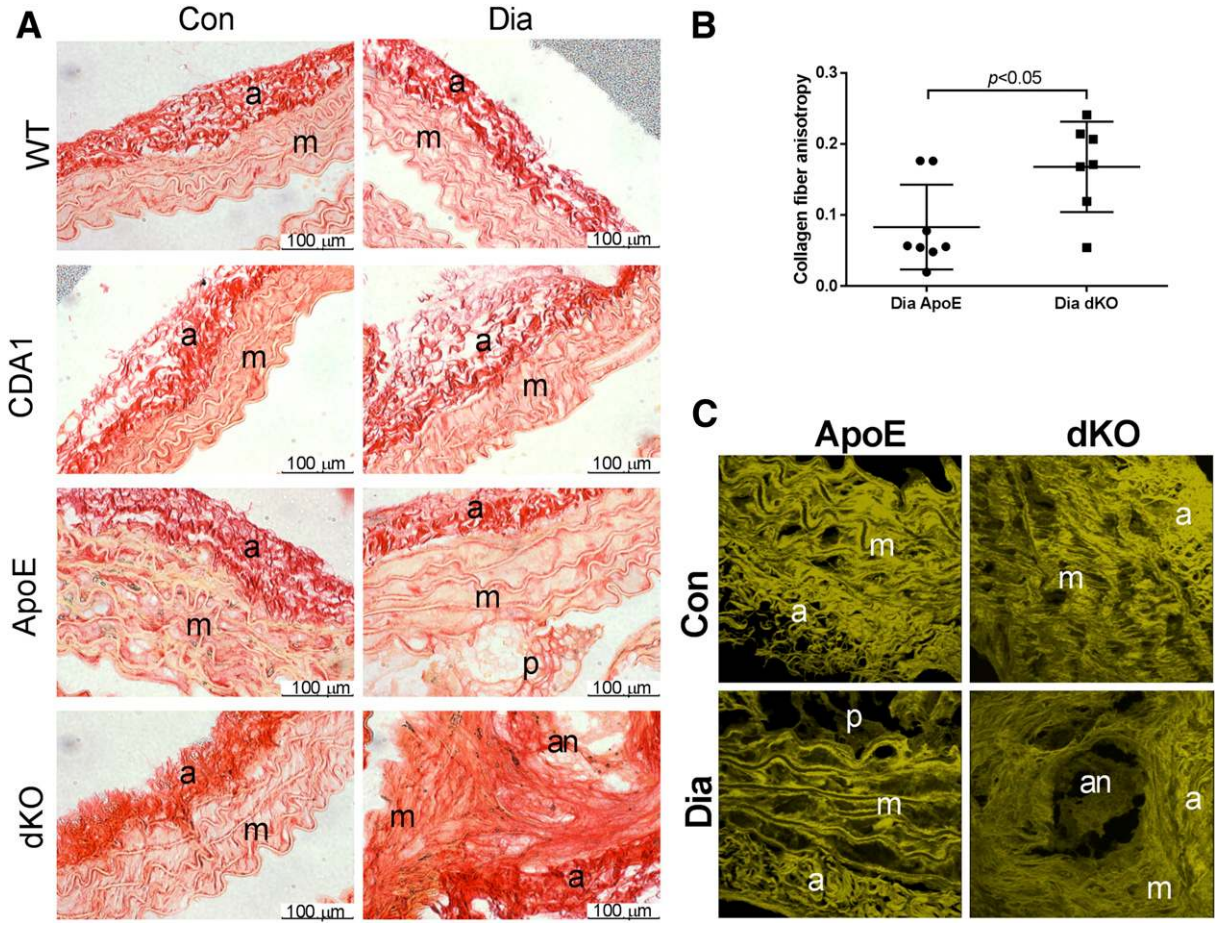

Figure 4—Picrosirius red–stained aortic sections examined by light microscopy show disorganized collagen fiber structures in the medial and adventitial layers of diabetic (Dia) dKO mouse aortas, particularly at the aneurysm sites in comparison with WT, CDA1 KO (CDA1), and ApoE KO (ApoE) groups (*A*). The collagen fiber orientation anisotropy quantitation at the sites of lesion in diabetic ApoE and dKO mice as determined using ImageJ software (National Institutes of Health) is shown (*B*). Collagen fiber organization, reconstructed from the backscatter confocal images of aortas from diabetic dKO mice, shows more disorganization than that from ApoE KO mice (*C*). a, adventitia; an, aneurysm site; Con, control; m, media; p, plaque.

whereas diabetic ApoE KO mice had a lower fatal rupture rate of 19% (4 out of 21) occurring on days 5, 7, 22, and 25 ($P < 0.05$) (Fig. 7*A*). This diabetes-associated protective effect on aneurysm-related mortality was not observed in AngII-infused dKO mice in which CDA1 had been deleted, with similar survival curves for both nondiabetic and diabetic dKO mice (Fig. 7*B*). Kaplan-Meier analysis of all four groups confirmed these findings. Nondiabetic ApoE KO mice had shorter estimated mean survival of 17.0 days (95% CI 12.0–22.1) than diabetic mice (25.3 days [95% CI 22.4–28.2]; $P = 0.029$, log-rank pairwise comparison), whereas nondiabetic and diabetic dKO mice had similar survivals (21.7 days [95% CI 17.4–26.0] vs. 24.7 days [95% CI 20.5–28.9]; $P = 0.39$). Comparison of nondiabetic ApoE KO and dKO groups showed no clear difference, which was confirmed by log-rank analysis of these groups alone ($P = 0.18$). These findings demonstrate that diabetes was associated with reduced severity of aortic aneurysms induced by an AngII infusion in ApoE KO mice and, importantly, that this phenomenon was CDA1 dependent.

In this model, most of the fatal aneurysm rupture occurred in the abdominal aorta with blood clot seen in the abdomen (Supplementary Figs. 5 and 6). Furthermore, there was a significantly enlarged diameter in the suprarenal region of aortas in these mice (Supplementary Figs. 5 and 6). Aneurysms were identified by the presence of aortic enlargement in 82% (14 out of 17) of nondiabetic and 60% (12 out of 20) of diabetic ApoE KO mice and similarly in 81% (17 out of 21) of nondiabetic dKO and 62% (8 out of 13) of diabetic dKO mice (Supplementary Figs. 5 and 6). These observations and the mortality data suggest that CDA1 does not affect the onset but rather the severity of aneurysm in this model.

AngII infusion caused suprarenal aortic expansion in both nondiabetic and diabetic ApoE KO mice (Fig. 7*C*), with aortic diameter determined by ultrasound (Supplementary Fig. 7). Baseline suprarenal aortic diameters had low individual variation within either nondiabetic or diabetic ApoE KO mice. Diabetic ApoE KO mice had a larger mean diameter at baseline than nondiabetic controls

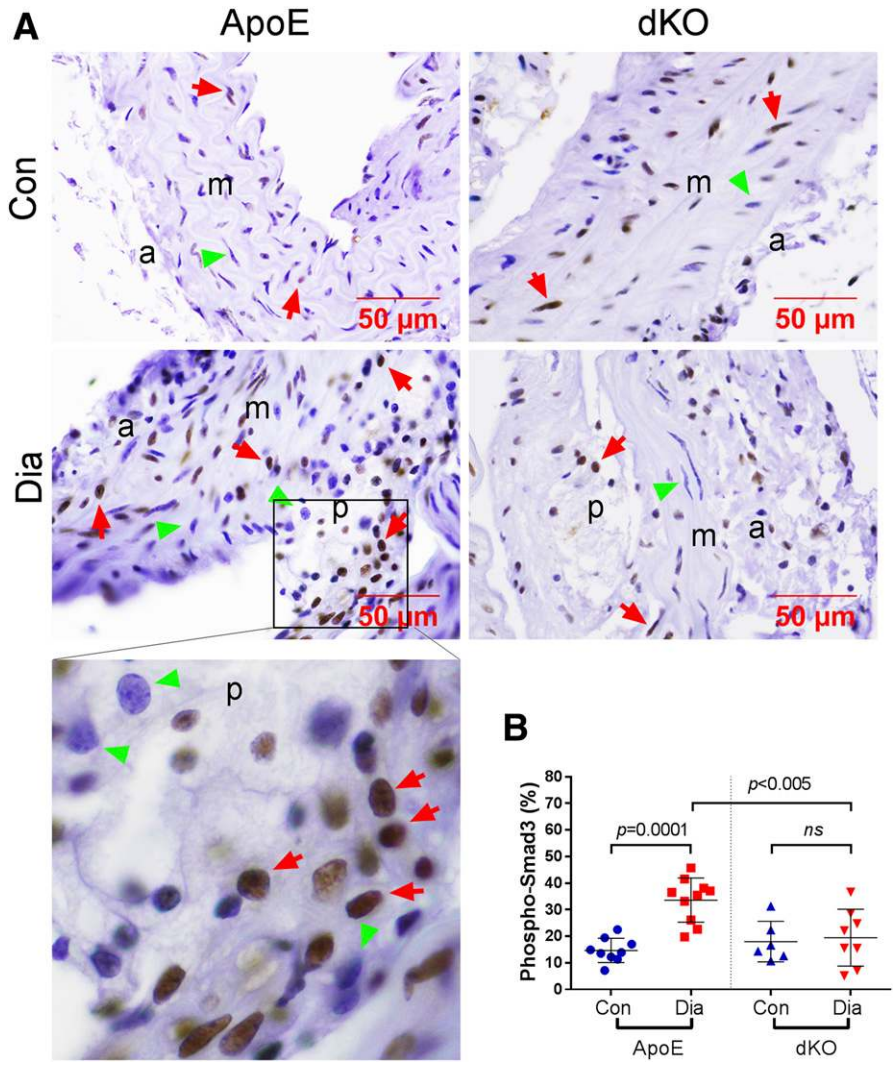

Figure 5—Aortic nuclear phospho-Smad3 staining is increased by diabetes in ApoE KO mice and is attenuated in diabetic dKO mice. Nuclear staining of phospho-Smad3 ($Ser^{433/435}$) detected by immunohistochemical staining (brown color) is shown in aortas from nondiabetic (Con) and 20-week diabetic (Dia) ApoE KO (ApoE) and dKO mice (*A*). A part of the ApoE Dia section (boxed) is shown as an enlarged image. Red arrows indicate positive staining; green arrowheads indicate negative staining. *B*: The phospho-Smad3 nuclear stained positive cells (%) are quantified and shown as univariate scatterplots with mean ± SD and *P* value between specified groups. a, adventitia; m, media; p, plaque.

(1.17 ± 0.03 vs. 1.03 ± 0.02 mm; $P < 0.05$) (Fig. 7*C*). After 1 week of AngII infusion, the mean diameters of both groups were significantly increased ($P < 0.001$) (Fig. 7*C*). All of the mice in the nondiabetic ApoE KO group had an enlarged aortic size, whereas some mice in the diabetic group had no change in aortic diameter (Fig. 7*C*). The aortic expansion rate at week 1 in response to AngII infusion was 161 ± 11 and 130 ± 7% ($P < 0.05$) in nondiabetic and diabetic ApoE KO mice, respectively (Fig. 7*E*).

At baseline, the suprarenal aortic diameter was larger in dKO mice with CDA1 deleted (1.29 ± 0.03 mm) than in ApoE KO mice (1.03 ± 0.02 mm) ($P < 0.001$) or diabetic dKO mice (1.1 ± 0.06 mm) ($P < 0.05$) (Fig. 7*D*). After 1 week of AngII infusion, mean suprarenal aortic diameters increased relative to those at baseline in both nondiabetic and diabetic dKO groups ($P < 0.05$) (Fig. 7*D*). Unlike ApoE KO mice, there was no difference in the aortic expansion rates between nondiabetic and diabetic dKO mice (126 ± 10 vs. 125 ± 11%) (Fig. 7*F*), demonstrating that the inhibitory effect of diabetes on aortic expansion in response to AngII, as observed in ApoE KO mice, was CDA1 dependent. This finding complements the aortic aneurysm rupture data (Fig. 7*A* and *B*) and indeed suggests that CDA1 per se mediates the protective effect of diabetes in reducing the severity of AngII-induced aneurysms in this model.

CDA1 Expression Was Downregulated in Human Subjects With AAA

In order to explore the clinical relevance of our primary findings from the preclinical studies, we examined the mRNA levels of CDA1 in 15 biopsy samples from human patients with AAA and 6 nonaneurysm control samples.

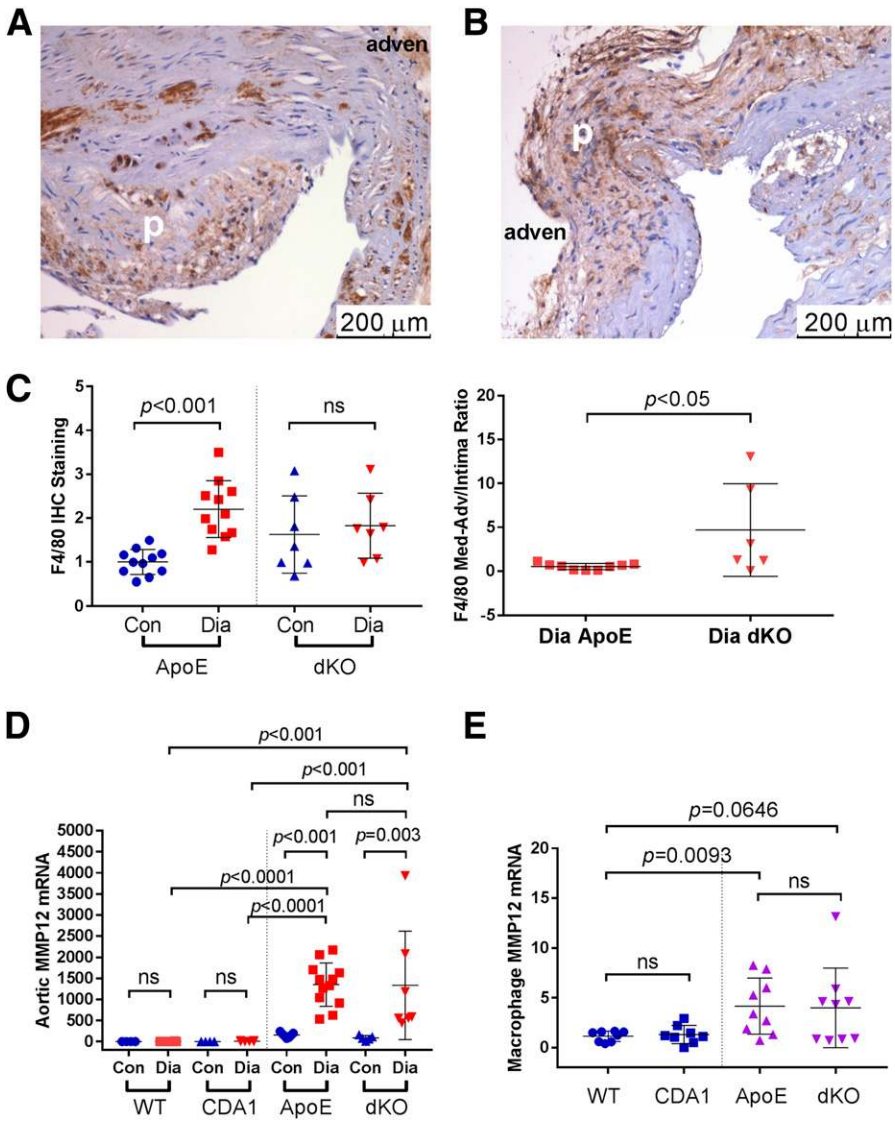

Figure 6—Macrophage infiltration and MMP12 expression are increased in 20-week diabetic mice with ApoE deficiency. *A–C*: Immunohistochemical (IHC) staining of the macrophage marker, F4/80, is shown in the aortic sections of diabetic ApoE KO (*A*) and dKO (*B*) mice. Atherosclerotic plaque (p) and adventitial side (adven) of aortic wall are indicated. Quantification of the staining is shown for control (Con) and diabetic (Dia) ApoE KO (ApoE) and dKO mice (*C*, left panel). The ratio of the medial-adventitial (Med-Adv) F4/80 staining to the intima staining at sites containing a plaque in Dia ApoE and dKO mice is also shown (*C*, right panel). MMP12 mRNA levels in aortas from Con and 20-week Dia WT, CDA1 KO (CDA1), ApoE, and dKO mice (*D*) as well as in macrophages (*E*) isolated from peritoneal cavity, using the method previously described (55), of ~12-week-old male WT, CDA1 KO, ApoE KO, and dKO mice were determined by RT-PCR. Data (*C–E*) are shown as univariate scatterplots with mean ± SD and *P* value between specified groups.

The majority of the patients with AAA were male (80%) and had dyslipidemia (73%). One-third of the patients with AAA were diabetic (33%). Their average maximum infrarenal aortic diameter was 58.9 ± 2.8 mm (mean ± SEM), with a trend toward a smaller diameter in subjects with diabetes (n = 5) than in subjects without diabetes (51.8 ± 5.1 mm [n = 5] vs. 62.5 ± 2.9 mm [n = 10]; P = 0.072). The average age of the AAA group was greater than that of the control samples from younger organ donors ($P < 0.001$), reflecting the fact that AAA is an age-related disease (Supplementary Table 4). As shown in Fig. 8, CDA1 gene expression in the AAA samples was downregulated ~70% when compared with the control subjects (P = 0.006). In patients with AAA, there was no difference in CDA1 expression levels between participants with diabetes and without diabetes (Fig. 8).

DISCUSSION

The current study reveals a potential molecular mechanism to explain, at least in part, the resistance to aneurysm formation in diabetes, a puzzling and previously poorly understood observation. Numerous studies have revealed

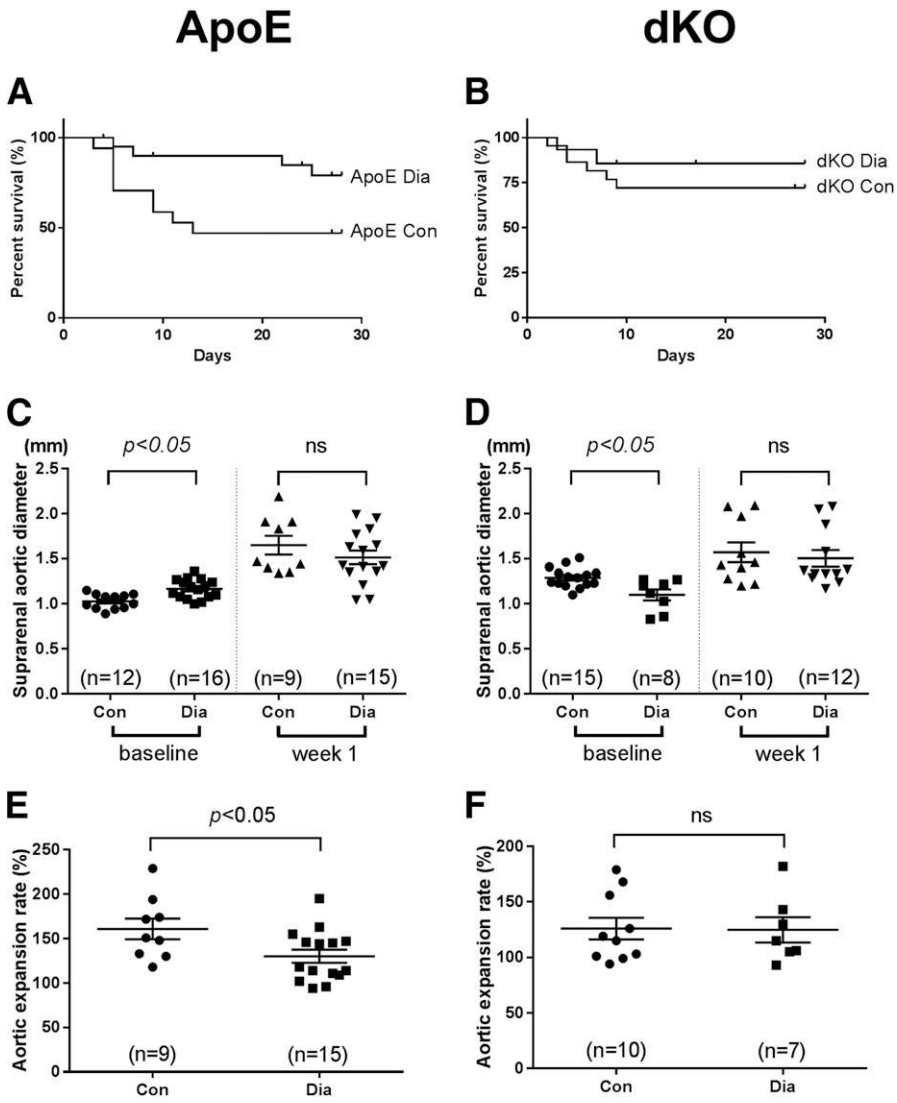

Figure 7—Diabetes reduces fatal aortic aneurysm rupture and aortic expansion in AngII-infused ApoE KO mice, which are CDA1 dependent. Percent survival (%) curves of control (Con) and diabetic (Dia) ApoE KO (*A*) and dKO (*B*) mice are shown with respect to days of AngII infusion. Animals killed for animal welfare reasons, including three diabetic ApoE KO, one nondiabetic dKO, and six diabetic dKO mice, were included in the survival curve (censored). Inner diameters of suprarenal aortas determined by ultrasound imaging at baseline and week 1 after AngII infusion are shown for Con and Dia ApoE KO (*C*) and dKO (*D*) mice. Suprarenal aortic expansion rates (%) at week 1 relative to the baseline are shown for Con and Dia ApoE KO (*E*) and dKO (*F*) mice. Individual value, group mean ± SEM, group size (*n*), and *P* value between specified groups are shown (*C–F*).

a decreased incidence of aneurysms in subjects with diabetes, as summarized in a recent meta-analysis (2). Interestingly, metformin, a widely used diabetes medication, has been observed to be associated with reduced AAA growth in patients who have diabetes (40,41). Whether this association is due to metformin alone or the effect of diabetes plus metformin is not clear and requires a randomized trial to resolve. In the current study, in which metformin was not administered, diabetic ApoE KO mice had less severe aneurysms than their nondiabetic controls. It appears likely that there are multiple mechanisms by which diabetes slows AAA growth, including the mechanisms highlighted in this study.

Diabetes is a state of enhanced fibrosis with increased ECM accumulation in the vasculature (7,23). We have previously shown increased renal and vascular expression of CDA1 in diabetes, which enhances TGF-β/Smad signaling, leading to increased ECM accumulation (23–25). Increased ECM accumulation presumably contributes to the relative protection against aneurysm formation in subjects with diabetes, although it is possible that multiple mechanisms are involved (2,6,12,42). It has been reported that subjects with diabetes with chronic complications are less likely to develop aortic aneurysms than patients with diabetes without complications (43). In this and in our previous studies (7,23), diabetic ApoE KO mice did not develop any

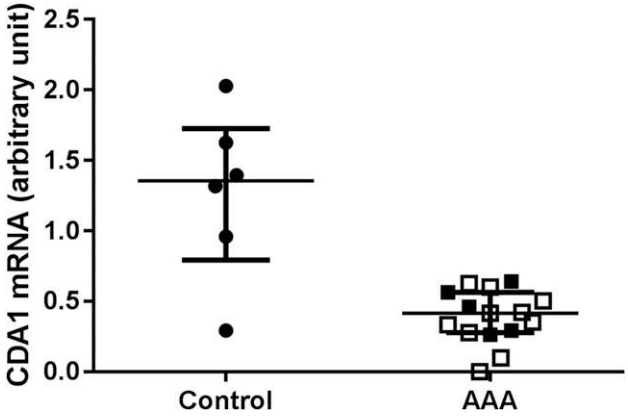

Figure 8—CDA1 mRNA levels are decreased in AAAs in humans. Aortas from 15 subjects with AAA and 6 organ donors as control subjects were examined for CDA1 mRNA levels by RT-PCR using β-actin as a housekeeping gene control. β-Actin was chosen as the housekeeping gene because analyses showed that its expression was similar in aortic biopsies from patients and organ donors. Individual results (relative value) are shown as dots in groups as well as the group median value with the interquartile range. Open squares represent 10 subjects without diabetes, and black squares represent 5 subjects with diabetes and AAA. Control group median is 1.356 (interquartile range 0.792–1.726) and AAA group median is 0.415 (interquartile range 0.279–0.564). $P = 0.006$.

aneurysms in the absence of classic stimuli of aneurysm formation, such as AngII infusion, and were found to have greater aortic phospho-Smad3 levels; greater accumulation of collagens I, III, and IV; and greater thickness of elastin lamella, which could reflect an increase in strength of the aortic wall. We have previously shown that aortic mRNA levels of CDA1 (the *Tspyl2* gene) are increased by approximately twofold at 10 weeks after diabetes induction in ApoE KO mice, which are further increased to greater than sixfold at 20 weeks after diabetes induction with concurrent increases in aortic CDA1 protein staining, TGF-β expression, and ECM accumulation (23). We have previously reported that CDA1 overexpression and CDA1 knockdown or genetic deletion of CDA1 enhances and attenuates TGF-β signaling, respectively, as reflected by changes in TGF-β–stimulated phosphorylation of Smad3 and TGF-β–responsive promoter luciferase reporter activities. This effect of CDA1 on TGF-β signaling is probably at least in part via influencing expression of TGF-β type I receptor (23–25). In this study, diabetic dKO mice in the absence of CDA1 showed attenuated TGF-β signaling, breakage of elastin lamella, and reduced ECM accumulation, which presumably would contribute to aneurysm formation (44,45). The effect of CDA1 on TGF-β signaling in the vascular smooth muscle cells has been previously described (23). Indeed, this finding is consistent with a recent report that impaired TGF-β signaling in the vascular smooth muscle cells causes aortic aneurysm formation in mice (22). This increase in aneurysm formation is reflected by the increased aortic diameter in diabetic dKO mice. This is potentially clinically relevant because TGF-β and other TGF-β–dependent molecules such as connective tissue growth factor remain targets for reducing other diabetic complications such as nephropathy in subjects with diabetes (11,46). The current study highlights the possibility that aggressive approaches to interrupt the TGF-β axis could lead to increased susceptibility to aneurysms.

As outlined earlier, numerous clinical studies, recently summarized in a meta-analysis (2), have demonstrated reduced aneurysms in subjects with type 2 diabetes (T2D). Indeed, our preclinical experiments are consistent with the clinical studies with reduced severity of aortic dilation in response to the proaneurysm stimulus, AngII, in diabetic mice. Although these studies have focused on an insulin-deficient model of diabetes, because aneurysms occur in the older population in whom T2D is more prevalent, it is worth considering subsequent studies in relevant models of T2D.

Runt-related transcription factor 2 (Runx2) is known to be upregulated by TGF-β (47) and is involved in calcification in the vasculature. Furthermore, recently, Runx2 was found to be upregulated in aortas of diabetic *db/db* mice in association with increased aortic fibrosis and stiffness (48). Whether CDA1 plays a role in affecting Runx2 in the vascular calcification and vascular fibrosis due to its ability to influence TGF-β signaling requires further investigation, although our experiments failed to show this phenomenon in our model (data not shown), which displays prominent aneurysm development rather than vascular calcification.

Macrophage activation and infiltration from the adventitia are common features observed in aneurysms (39,49). Macrophages were mainly located within the atherosclerotic plaque specifically within the intimal layer of the aorta in the diabetic ApoE KO mice. By contrast, in diabetic dKO mice, macrophages infiltrated into the medial and adventitial layers with associated increased elastin breakage in the medial layer and collagen structural damage in both medial and adventitial layers. This finding is consistent with the macrophage distribution pattern previously reported in other models of aneurysm formation (50,51), which is associated with increased elastin fiber digestion and aneurysm or dissection formation (34,39,49,52). The mechanisms responsible for the differential distribution patterns of macrophages within the aortas in diabetic ApoE KO and diabetic dKO mice are still unclear. It is yet to be determined whether CDA1 deficiency–related ECM remodeling is responsible for the aortic wall becoming more prone to the widespread macrophage infiltration into the media and adventitial layers.

Therefore, this study suggests the importance of inflammation and the attenuation of profibrotic pathways in the pathogenesis of aortic aneurysm. Deletion of CDA1, a molecule closely linked to the TGF-β axis, led to enhanced aneurysm formation in the context of the generally profibrotic milieu of diabetes. The role of the TGF-β axis in aneurysm formation has been extensively explored, with a large body of experimental and clinical data (14–21,53) emphasizing

that dysregulation of this pathway, both enhanced and reduced TGF-β signaling, is associated with aneurysm formation.

Based on the results of our studies, part of the protective role of diabetes in the pathogenesis of aneurysms is postulated to be mediated by CDA1. Indeed, AngII infusion caused development of severe AAA mainly in the suprarenal region of aortas in ApoE KO and dKO mice, as reflected by rapid death due to aortic aneurysm rupture within a few days and significant expansion of the suprarenal aorta in response to AngII. These parameters were significantly attenuated in the diabetic ApoE KO mice. By contrast, diabetic CDA1-deficient dKO mice failed to show attenuation of these parameters when compared with their nondiabetic dKO counterparts. Thus, these findings clearly demonstrate a role for CDA1 in mediating the protective effect of diabetes on aneurysms. Because the occurrence rate of aneurysm was similar in both ApoE KO and dKO mice, it appears that CDA1 reduces aneurysm severity, but not the formation of aneurysms in this model. This is consistent with the notion that CDA1 promotes the TGF-β/Smad/ECM pathway, leading to increased accumulation of ECMs in the vasculature in diabetes (23), hence limiting the growth of the aneurysms induced by AngII.

In this study, the two mouse strains (ApoE KO and dKO) appeared to differ in response to the AngII infusion, as reflected by a trend toward higher survival and less aortic expansion in dKO mice, albeit these differences are not statistically significant, probably due to a small group size. A comparison between the nondiabetic and diabetic littermates of ApoE KO mice showed a diabetes-associated protection in the AngII infusion groups with respect to fatality and aortic expansion (Fig. 7*A* and *E*). This phenomenon of diabetes-associated protection of aneurysm development was not seen in the dKO groups (Fig. 7*B* and *F*). Use of a CDA1-transgenic mouse strain to overexpress CDA1 in relevant vascular cells or a pharmacological enhancer of CDA1, if available, would be very useful to confirm the role of CDA1 in protecting aneurysm development in this animal model.

The potential clinical relevance of these preclinical findings was explored, and CDA1 expression was found to be reduced ~70% in human AAA samples when compared with control subjects without AAA. These AAA samples have been previously shown to have reduced expression of the TGF-β type II receptor (21). This is consistent with our previous experimental results that CDA1 deficiency was associated with decreased TGF-β signaling (23–25). This finding in humans supports the potential likelihood that CDA1 plays a protective role in human aneurysms. We have previously described that CDA1 expression is increased in experimental atherosclerosis in a model without aneurysms (23) and found that CDA1 was strongly stained in human atherosclerotic plaques (A. Dai, Z. Chai, unpublished observation). These findings may reflect distinct roles for CDA1 in vascular ECM remodeling and the obviously different pathogenic factors involved in the development of atherosclerosis and aneurysms (54). In this study, subjects with diabetes with AAA had reduced CDA1 gene expression consistent with CDA1 playing a key protective role in aneurysm formation in those individuals who are susceptible to this condition. With limited availability of appropriate human aneurysmal tissue, protein levels of CDA1 could not be measured, and this is a limitation of this study.

In conclusion, this study demonstrated that CDA1-deficient mice with concurrent diabetes developed aneurysms, but diabetic mice in the presence of CDA1 were protected from severe aneurysms. With evidence of reduced CDA1 expression in human AAA, these findings are consistent with the postulate that CDA1 may play a protective role against aneurysm formation. Our findings suggest that CDA1 may be a therapeutic target to prevent or retard the progression of human aneurysms and that this protein may play a key role in explaining the clinical observation that subjects with diabetes are less susceptible to aneurysm formation.

Acknowledgments. The authors thank Samantha Sacca (Baker IDI Heart and Diabetes Institute) for assistance with animal studies. Organ donors and next of kin (Donate Life in Queensland) are gratefully acknowledged. Sadly, Philip Walker died during the final preparation of the manuscript, and the authors are indebted to his untiring work and leadership on this and other vascular research.

Funding. This study was supported by the National Health and Medical Research Council (NHMRC) and the National Heart Foundation of Australia. M.E.C. is an NHMRC Senior Principal Research Fellow, X.-J.D. is an NHMRC senior research fellow, and J.G. is a Practitioner Fellow. J.G. holds a Senior Clinical Research Fellowship from the Health and Medical Research Office, Queensland, Australia. M.N. is supported by the Prince Charles Hospital Foundation, Brisbane, Queensland, Australia.

Duality of Interest. No potential conflicts of interest relevant to this article were reported.

Author Contributions. J.L. performed the 20-week diabetes animal study. J.L. and Z.C. wrote the manuscript. P.H., A.D., and T.W. performed the AngII infusion animal study. Y.T. and B.C. were involved in animal tissue collection and analysis. H.K. and X.-J.D. carried out ultrasound imaging. X.-J.D., L.A.B., J.L.W.-B., J.G., T.J.A., and M.E.C. read and critically edited the manuscript. L.A.B. analyzed survival curve data. E.B. performed analysis of human biopsy samples. P.W., M.N., M.W., and J.G. organized collection of human samples and data. Z.C. designed and initiated the experiments. Z.C. is the guarantor of this work and, as such, had full access to all of the data in the study and takes responsibility for the integrity of the data and the accuracy of the data analysis.

References

1. Moxon JV, Parr A, Emeto TI, Walker P, Norman PE, Golledge J. Diagnosis and monitoring of abdominal aortic aneurysm: current status and future prospects. Curr Probl Cardiol 2010;35:512–548

2. Shantikumar S, Ajjan R, Porter KE, Scott DJ. Diabetes and the abdominal aortic aneurysm. Eur J Vasc Endovasc Surg 2010;39:200–207

3. Lederle FA, Johnson GR, Wilson SE, et al.; Aneurysm Detection and Management (ADAM) Veterans Affairs Cooperative Study Group. Prevalence and associations of abdominal aortic aneurysm detected through screening. Ann Intern Med 1997;126:441–449

4. Blanchard JF, Armenian HK, Friesen PP. Risk factors for abdominal aortic aneurysm: results of a case-control study. Am J Epidemiol 2000;151:575–583

5. Karanjia PN, Madden KP, Lobner S. Coexistence of abdominal aortic aneurysm in patients with carotid stenosis. Stroke 1994;25:627–630

6. Golledge J, Karan M, Moran CS, et al. Reduced expansion rate of abdominal aortic aneurysms in patients with diabetes may be related to aberrant monocyte-matrix interactions. Eur Heart J 2008;29:665–672

7. Candido R, Jandeleit-Dahm KA, Cao Z, et al. Prevention of accelerated atherosclerosis by angiotensin-converting enzyme inhibition in diabetic apolipoprotein E-deficient mice. Circulation 2002;106:246–253
8. Ruiz-Ortega M, Rodríguez-Vita J, Sanchez-Lopez E, Carvajal G, Egido J. TGF-beta signaling in vascular fibrosis. Cardiovasc Res 2007;74:196–206
9. Ziyadeh FN, Hoffman BB, Han DC, et al. Long-term prevention of renal insufficiency, excess matrix gene expression, and glomerular mesangial matrix expansion by treatment with monoclonal antitransforming growth factor-beta antibody in db/db diabetic mice. Proc Natl Acad Sci U S A 2000;97:8015–8020
10. Petersen M, Thorikay M, Deckers M, et al. Oral administration of GW788388, an inhibitor of TGF-beta type I and II receptor kinases, decreases renal fibrosis. Kidney Int 2008;73:705–715
11. McGowan TA, Zhu Y, Sharma K. Transforming growth factor-beta: a clinical target for the treatment of diabetic nephropathy. Curr Diab Rep 2004;4:447–454
12. Norman PE, Davis TM, Le MT, Golledge J. Matrix biology of abdominal aortic aneurysms in diabetes: mechanisms underlying the negative association. Connect Tissue Res 2007;48:125–131
13. Didangelos A, Yin X, Mandal K, et al. Extracellular matrix composition and remodeling in human abdominal aortic aneurysms: a proteomics approach. Mol Cell Proteomics 2011;10:M111.008128
14. Boileau C, Guo DC, Hanna N, et al.; National Heart, Lung, and Blood Institute (NHLBI) Go Exome Sequencing Project. TGFB2 mutations cause familial thoracic aortic aneurysms and dissections associated with mild systemic features of Marfan syndrome. Nat Genet 2012;44:916–921
15. Lindsay ME, Schepers D, Bolar NA, et al. Loss-of-function mutations in TGFB2 cause a syndromic presentation of thoracic aortic aneurysm. Nat Genet 2012;44:922–927
16. Pannu H, Fadulu VT, Chang J, et al. Mutations in transforming growth factor-beta receptor type II cause familial thoracic aortic aneurysms and dissections. Circulation 2005;112:513–520
17. Loeys BL, Schwarze U, Holm T, et al. Aneurysm syndromes caused by mutations in the TGF-beta receptor. N Engl J Med 2006;355:788–798
18. van de Laar IM, Oldenburg RA, Pals G, et al. Mutations in SMAD3 cause a syndromic form of aortic aneurysms and dissections with early-onset osteoarthritis. Nat Genet 2011;43:121–126
19. Holm TM, Habashi JP, Doyle JJ, et al. Noncanonical TGFβ signaling contributes to aortic aneurysm progression in Marfan syndrome mice. Science 2011;332:358–361
20. Loeys BL, Chen J, Neptune ER, et al. A syndrome of altered cardiovascular, craniofacial, neurocognitive and skeletal development caused by mutations in TGFBR1 or TGFBR2. Nat Genet 2005;37:275–281
21. Biros E, Walker PJ, Nataatmadja M, West M, Golledge J. Downregulation of transforming growth factor, beta receptor 2 and Notch signaling pathway in human abdominal aortic aneurysm. Atherosclerosis 2012;221:383–386
22. Zhang P, Hou S, Chen J, et al. Smad4 deficiency in smooth muscle cells initiates the formation of aortic aneurysm. Circ Res 2016;118:388–399
23. Pham Y, Tu Y, Wu T, et al. Cell division autoantigen 1 plays a profibrotic role by modulating downstream signalling of TGF-beta in a murine diabetic model of atherosclerosis. Diabetologia 2010;53:170–179
24. Tu Y, Wu T, Dai A, et al. Cell division autoantigen 1 enhances signaling and the profibrotic effects of transforming growth factor-β in diabetic nephropathy. Kidney Int 2011;79:199–209
25. Chai Z, Dai A, Tu Y, et al. Genetic deletion of cell division autoantigen 1 retards diabetes-associated renal injury. J Am Soc Nephrol 2013;24:1782–1792
26. Rush C, Nyara M, Moxon JV, Trollope A, Cullen B, Golledge J. Whole genome expression analysis within the angiotensin II-apolipoprotein E deficient mouse model of abdominal aortic aneurysm. BMC Genomics 2009;10:298
27. Daugherty A, Cassis LA. Mouse models of abdominal aortic aneurysms. Arterioscler Thromb Vasc Biol 2004;24:429–434
28. Xu Q, Chakravorty A, Bathgate RA, Dart AM, Du XJ. Relaxin therapy reverses large artery remodeling and improves arterial compliance in senescent spontaneously hypertensive rats. Hypertension 2010;55:1260–1266
29. Xiao J, Angsana J, Wen J, et al. Syndecan-1 displays a protective role in aortic aneurysm formation by modulating T cell-mediated responses. Arterioscler Thromb Vasc Biol 2012;32:386–396
30. Sun J, Sukhova GK, Yang M, et al. Mast cells modulate the pathogenesis of elastase-induced abdominal aortic aneurysms in mice. J Clin Invest 2007;117:3359–3368
31. Soro-Paavonen A, Watson AM, Li J, et al. Receptor for advanced glycation end products (RAGE) deficiency attenuates the development of atherosclerosis in diabetes. Diabetes 2008;57:2461–2469
32. Dolber PC, Spach MS. Conventional and confocal fluorescence microscopy of collagen fibers in the heart. J Histochem Cytochem 1993;41:465–469
33. Boudaoud A, Burian A, Borowska-Wykręt D, et al. FibrilTool, an ImageJ plug-in to quantify fibrillar structures in raw microscopy images. Nat Protoc 2014;9:457–463
34. Daugherty A, Manning MW, Cassis LA. Angiotensin II promotes atherosclerotic lesions and aneurysms in apolipoprotein E-deficient mice. J Clin Invest 2000;105:1605–1612
35. Barisione C, Charnigo R, Howatt DA, Moorleghen JJ, Rateri DL, Daugherty A. Rapid dilation of the abdominal aorta during infusion of angiotensin II detected by noninvasive high-frequency ultrasonography. J Vasc Surg 2006;44:372–376
36. Parr A, Buttner P, Shahzad A, Golledge J. Relation of infra-renal abdominal aortic calcific deposits and cardiovascular events in patients with peripheral artery disease. Am J Cardiol 2010;105:895–899
37. Parr A, McCann M, Bradshaw B, Shahzad A, Buttner P, Golledge J. Thrombus volume is associated with cardiovascular events and aneurysm growth in patients who have abdominal aortic aneurysms. J Vasc Surg 2011;53:28–35
38. Golledge J, Clancy P, Jamrozik K, Norman PE. Obesity, adipokines, and abdominal aortic aneurysm: Health in Men study. Circulation 2007;116:2275–2279
39. Curci JA, Liao S, Huffman MD, Shapiro SD, Thompson RW. Expression and localization of macrophage elastase (matrix metalloproteinase-12) in abdominal aortic aneurysms. J Clin Invest 1998;102:1900–1910
40. Fujimura N, Xiong J, Kettler EB, et al. Metformin treatment status and abdominal aortic aneurysm disease progression. J Vasc Surg 2016;64:46–54.e8
41. Golledge J, Moxon J, Pinchbeck J, et al. Association between metformin prescription and growth rates of abdominal aortic aneurysms. Br J Surg 2017;104:1486–1493
42. Torsney E, Pirianov G, Cockerill GW. Diabetes as a negative risk factor for abdominal aortic aneurysm - does the disease aetiology or the treatment provide the mechanism of protection? Curr Vasc Pharmacol 2013;11:293–298
43. Prakash SK, Pedroza C, Khalil YA, Milewicz DM. Diabetes and reduced risk for thoracic aortic aneurysms and dissections: a nationwide case-control study. J Am Heart Assoc 2012;1:e000323
44. Wang Y, Ait-Oufella H, Herbin O, et al. TGF-beta activity protects against inflammatory aortic aneurysm progression and complications in angiotensin II-infused mice. J Clin Invest 2010;120:422–432
45. Campa JS, Greenhalgh RM, Powell JT. Elastin degradation in abdominal aortic aneurysms. Atherosclerosis 1987;65:13–21
46. Yanagita M. Inhibitors/antagonists of TGF-β system in kidney fibrosis. Nephrol Dial Transplant 2012;27:3686–3691
47. Lee KS, Hong SH, Bae SC. Both the Smad and p38 MAPK pathways play a crucial role in Runx2 expression following induction by transforming growth factor-beta and bone morphogenetic protein. Oncogene 2002;21:7156–7163
48. Raaz U, Schellinger IN, Chernogubova E, et al. Transcription factor Runx2 promotes aortic fibrosis and stiffness in Type 2 diabetes mellitus. Circ Res 2015;117:513–524
49. Shipley JM, Wesselschmidt RL, Kobayashi DK, Ley TJ, Shapiro SD. Metalloelastase is required for macrophage-mediated proteolysis and matrix invasion in mice. Proc Natl Acad Sci USA 1996;93:3942–3946
50. Saraff K, Babamusta F, Cassis LA, Daugherty A. Aortic dissection precedes formation of aneurysms and atherosclerosis in angiotensin II-infused, apolipoprotein E-deficient mice. Arterioscler Thromb Vasc Biol 2003;23:1621–1626
51. Rateri DL, Howatt DA, Moorleghen JJ, Charnigo R, Cassis LA, Daugherty A. Prolonged infusion of angiotensin II in apoE(-/-) mice promotes macrophage

recruitment with continued expansion of abdominal aortic aneurysm. Am J Pathol 2011;179:1542–1548
52. Daugherty A, Manning MW, Cassis LA. Antagonism of AT2 receptors augments angiotensin II-induced abdominal aortic aneurysms and atherosclerosis. Br J Pharmacol 2001;134:865–870
53. Nataatmadja M, West M, West J, et al. Abnormal extracellular matrix protein transport associated with increased apoptosis of vascular smooth muscle cells in marfan syndrome and bicuspid aortic valve thoracic aortic aneurysm. Circulation 2003;108(Suppl. 1):II329–II334
54. Golledge J, Norman PE. Atherosclerosis and abdominal aortic aneurysm: cause, response, or common risk factors? Arterioscler Thromb Vasc Biol 2010;30:1075–1077
55. Zhang X, Goncalves R, Mosser DM. The isolation and characterization of murine macrophages. Curr Protoc Immunol 2008;Chapter 14:Unit 14.1